

# Long-Range Triplet Supercurrents Induced by Singlet Supercurrents Parallel to Magnetic Interfaces

Mohammad Alidoust<sup>1,2,\*</sup> and Klaus Halterman<sup>3,†</sup>

<sup>1</sup>*Department of Physics, University of Basel, Klingelbergstrasse 82, CH-4056 Basel, Switzerland*

<sup>2</sup>*Department of Physics, Faculty of Sciences, University of Isfahan, Hezar Jerib Avenue, Isfahan 81746-73441, Iran*

<sup>3</sup>*Michelson Lab, Physics Division, Naval Air Warfare Center, China Lake, California 93555, USA*

(Dated: March 2, 2024)

Employing a spin-parameterized Keldysh-Usadel technique for the diffusive regime, we demonstrate that even in the low proximity limit, considerable long-ranged triplet supercurrents can be effectively generated by spin-singlet supercurrents flowing *parallel* to the interfaces of uniform double ferromagnet interlayers with noncollinear exchange fields “*independent*” of actual junction geometry. The triplet supercurrents are found to be most pronounced when the thicknesses of the ferromagnet strips are unequal. To experimentally verify this generic phenomenon, we propose an accessible and well-controlled structure that can fully isolate the long-range triplet effects.

PACS numbers: 74.50.+r, 74.25.Ha, 74.78.Na, 74.50.+r, 74.45.+c

Spin carriers play a crucial role in spintronics devices where the spin of the carriers are used to transport or store information [1]. The spin current in diffusive ferromagnets due to spin-polarized charged carriers has a short-range propagation and limited spin coherence, thus presenting a detriment to the functionality of most spintronics devices [2]. This obstacle, however, can be resolved within the cryogenic realm by utilizing ferromagnetic (*F*)/superconductor (*S*) hybrids to generate spin polarized superconducting correlations that can propagate over several hundred nanometers with limited decay [3–6]. The induced spin-triplet odd-frequency superconducting correlations were theoretically predicted [6] for systems comprised of an *s*-wave superconductor in proximity to a ferromagnet. The signatures of such long-range proximity superconducting spin correlations were found shortly thereafter in experiments [7]. Numerous works since then, both experimentally and theoretically, have been devoted to the study and generation of superconducting correlations with net spin [8–12].

It has been shown that it is possible to study long-range supercurrents in *ballistic* bilayer [13] and *diffusive* trilayer [8] magnetic Josephson junctions where the supercurrent flows transversely relative to the noncollinear *F/F* interfaces. The situation is unfavorable however in the *low proximity* limit [14] where only faint signatures of the triplet supercurrents with spin projection  $m=\pm 1$  on the quantization axis exist, even in uniformly magnetized trilayers [8, 14]. The low proximity limit is realized for low transparency *S/F* interfaces, strongly magnetized layers, thick *F* barriers, and temperatures near the superconducting critical temperature, which prevails in many experiments [4, 6]. Thus, it is of considerable interest to determine the most simple and generic situations that permit generation of long-range triplet supercurrents in the low proximity limit. Moreover, the findings in this limit may pave the way for more pronounced triplet generation in similar structures within the ballistic and full proximity limit of diffusive regime [4, 6].

In this Letter, we demonstrate that by considering singlet

supercurrent flow “parallel” rather than “transverse” to the *F/F* interfaces, substantial long-range triplet supercurrents can be induced *regardless* of actual configuration and geometry [9, 12]. We make use of the two-dimensional quasiclassical Keldysh-Usadel approach in configuration-space, which is a general formalism appropriate for inhomogeneous diffusive *F/S* heterostructures containing generic magnetization and external magnetic field profiles [15, 16]. This two-dimensional approach is capable of explorations previously unattainable in strictly one-dimensional systems. A spin-parametrization technique is also incorporated within our method to pinpoint the behavior of the odd- and even-frequency components of the total supercurrent. To demonstrate the *generality* of our findings, we consider a variety of structures [9, 12] and specifically establish clear insights into the spatial profiles of singlet/triplet supercurrents in three different magnetic structures that host parallel supercurrent flow: A noncollinear double  $F_1/F_2$  interlayer that is either vertically [Fig. 1(a)] or horizontally [Fig. 1(b)] stacked between two *S* electrodes, or one that is horizontally sandwiched between a superconducting electrode and a finite sized normal metal [Fig. 1(c)]. In order to have supercurrent flow parallel to the  $F_1/F_2$  interfaces in the two latter structures, we introduce an externally applied magnetic field normal to the junction plane. The structures reveal that short-range spin-singlet supercurrents flowing parallel to the *F/F* interfaces containing noncollinear magnetizations and unequal thicknesses are effectively converted into long-ranged spin-triplet supercurrents. The simple structure shown in Fig. 1(c), permits experimental isolation of the long-range triplets and confirmation of this generic effect.

A general three-dimensional quasiclassical formalism for diffusive magnetic heterostructures subject to an external magnetic field is described by the following Usadel equations [15–17]:

$$D[\partial, \check{G}[\partial, \check{G}]] + i[\varepsilon + \text{diag}[\vec{h} \cdot \vec{\tau}, (\vec{h} \cdot \vec{\tau})^T], \check{G}] = 0, \quad (1)$$

in which the Pauli matrices constitute the components of

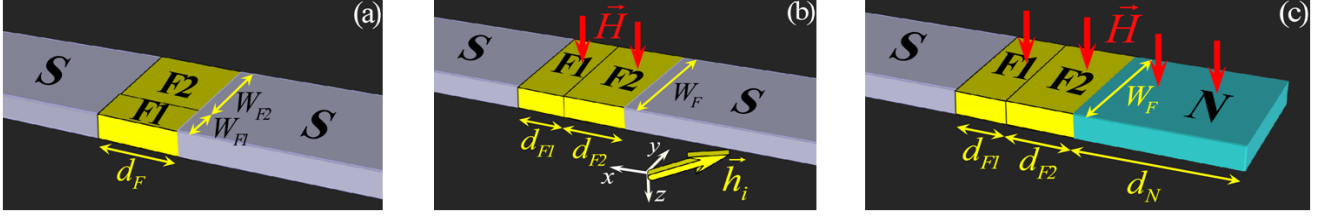


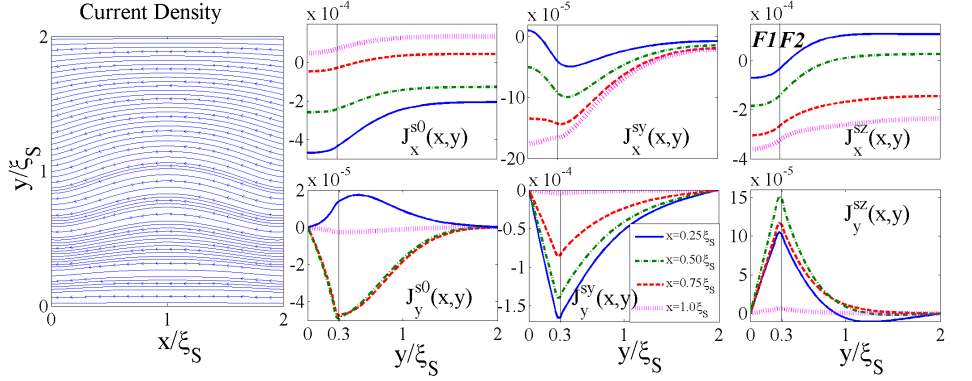
FIG. 1. Schematic of the proposed experimental setups of the basic  $F/S$  hybrid structures supporting supercurrent parallel to the  $F_1/F_2$  interfaces. The ferromagnetic layers,  $F_1$  and  $F_2$  have uniform magnetizations and  $N$  represents a nonmagnetic normal metal with a finite thickness  $d_N$ . Superconductivity is induced via  $s$ -wave superconducting terminals of infinite extent (labeled  $S$ ). We denote the exchange field of each  $F$  layer by  $\vec{h}_i = (h_i^x, h_i^y, h_i^z) = h_0(\sin \beta_i \cos \alpha_i, \sin \beta_i \sin \alpha_i, \cos \beta_i)$ , in which  $\beta_i$  and  $\alpha_i$  are spherical angles for  $i=1, 2$ . The junctions are located in the  $xy$  plane and the  $S/F$  interfaces are along the  $y$ -axis. In panel (a) the interface of the double ferromagnet region is oriented perpendicular to the  $S/F$  interfaces creating a two-dimensional hybrid. The widths of the rectangular  $F$  strips  $W_{F1}$ , and  $W_{F2}$  are generally different, while their lengths,  $d_F$ , are equal. In (b) and (c) all interfaces are parallel to the  $y$  axis. The widths of the rectangular  $F$  strips,  $W_F$ , are the same while the length of each magnetic layer,  $d_{F1}$  and  $d_{F2}$ , are not necessarily equal. To generate a supercurrent flowing along the  $F_1/F_2$  interface, an external magnetic field  $\vec{H}$  is directed along the  $z$ -axis, normal to the junction plane.

$\vec{\tau}$ . We denote the diffusion constant of the medium by  $D$  and  $\vec{G}$ ,  $\vec{h}$  are functions of coordinates  $\mathbf{r} \equiv (x, y, z)$  [15, 16]. Here, the exchange field describing the ferromagnetic region,  $\vec{h}(\mathbf{r}) = (h^x(\mathbf{r}), h^y(\mathbf{r}), h^z(\mathbf{r}))$ , can take arbitrary directions. We have defined a  $4 \times 4$  partial derivative matrix,  $\vec{\partial}$ , as  $\vec{\partial} \equiv \vec{\nabla} \hat{1} - ie \vec{A}(\mathbf{r}) \vec{\rho}_3$ , in which  $\vec{A}$  is the vector potential of the applied magnetic field,  $\vec{H}$ . The energy,  $\varepsilon$ , of the quasiparticles is measured from the Fermi surface  $\varepsilon_F$ . The resultant sixteen coupled complex partial differential equations should be supplemented by the appropriate boundary conditions to properly capture the electronic and transport characteristics of  $F/S$  hybrid structures. We employ the Kupriyanov-Lukichev boundary conditions at the  $S/F$  interfaces [18] and the induced proximity correlations are tuned by the barrier resistance  $\zeta$ :  $\zeta(\vec{G} \vec{\partial} \vec{G}) \cdot \hat{n} = [\vec{G}_{\text{BCS}}, \vec{G}]$ , in which  $\hat{n}$  is a unit vector normal to the interfaces and  $\vec{G}_{\text{BCS}}$  is the superconducting bulk solution. Under equilibrium conditions, the vector current density is expressed as an integration of the Keldysh block,  $\vec{J}(\mathbf{r}) = J_0 \int d\varepsilon \text{Tr} \{ \rho_3 (\vec{G} [\vec{\partial}, \vec{G}])^K \}$ , where  $J_0 = N_0 e D / 4$ ,  $N_0$  is the density of states at the Fermi surface, and  $e$  is the electron charge. To gain insight into the triplet supercurrent components, we use the spin-parametrization scheme for the Green's function [6]. Therefore, the anomalous component of the Green's function takes the following form in terms of the even ( $\mathbb{S}$ ) and odd ( $\mathbb{T}$ ) frequency parts:  $F(\mathbf{r}, \varepsilon) = i[\mathbb{S}(\mathbf{r}, \varepsilon) + \vec{\mathbb{T}}(\mathbf{r}, \varepsilon) \cdot \vec{\tau}] \tau_y$ , where  $\vec{\mathbb{T}}(\mathbf{r}, \varepsilon) \equiv (\mathbb{T}_x, \mathbb{T}_y, \mathbb{T}_z)$ , and  $\mathbb{T}_x, \mathbb{T}_y$  have  $m = \pm 1$  projections along the quantization axis, while  $\mathbb{T}_z$  has  $m = 0$  [6]. If we now substitute this decomposition into the Usadel equation, Eq. (1), we are able to separate the contributions  $\mathbb{S}$ ,  $\mathbb{T}_x$ ,  $\mathbb{T}_y$ , and  $\mathbb{T}_z$  to the charge supercurrent. To study the precise behavior of individual components constituting the Josephson current, we introduce the following decomposition scheme for the current density:  $J_{x,y} = J_{x,y}^{s0} + J_{x,y}^{sx} + J_{x,y}^{sy} + J_{x,y}^{sz}$ , where  $J_{x,y}^{s0}$  encompasses the  $\mathbb{S}$  terms, and  $J_{x,y}^{s\gamma}$  the  $\mathbb{T}_\gamma$  terms (designating  $\gamma = x, y, z$ ). Our formalism allows for arbitrary magnetization orientation in each ferromagnetic wire. However to most effectively realize the long-range behavior of the decomposed charge su-

percurrent, we take the magnetizations in the  $F_1$  and  $F_2$  wires to be orthogonal [6], with exchange fields  $\vec{h}_1 = (0, h^y, 0)$ , and  $\vec{h}_2 = (0, 0, h^z)$  or equivalently;  $\beta_1 = \alpha_1 = \pi/2$ , and  $\beta_2 = 0$ . We focus here on uniform  $F_1/F_2$  bilayers (the least and simplest layered structure) with  $F_1$  and  $F_2$  having unequal thicknesses as this results in more pronounced singlet-triplet conversion [14]. The magnitude of the exchange field in each ferromagnet is typically set at  $|\vec{h}_i| = 10\Delta_0$ , the temperature  $T$  corresponds to  $T = 0.05T_c$ , and  $\zeta = 4$ . The energies are normalized by the superconducting gap at zero temperature,  $\Delta_0$ , and the lengths by the superconducting coherence length,  $\xi_S$ .

To have absolute comparisons, we constrain the rectangular  $F$  strips to have equal total lengths and widths, i.e.,  $d_F = d_{F1} + d_{F2} = 2.0\xi_S$  and  $W_F = W_{F1} + W_{F2} = 2.0\xi_S$ , respectively (see Fig. 1). The  $S$  electrodes are given a macroscopic phase difference of  $|\varphi| = \pi/2$ , which is the phase difference corresponding to the critical supercurrent. In Fig. 2 we show results corresponding to the setup in Fig. 1(a) with  $W_{F1} = 0.3\xi_S$ ,  $W_{F2} = 1.7\xi_S$ , and no applied magnetic field. First, the spatial map of the total maximum charge supercurrent density shows that the current in the vicinity of the  $F_1/F_2$  junction has a nonzero  $y$ -component [19] (as mentioned earlier,  $y/\xi_S = 0.3$  coincides with the width of the  $F_1$  nano-wire,  $W_{F1} = 0.3\xi_S$ ). This result can be compared with Fig. 3(a) for an  $S/F_1/F_2/S$  junction with transverse supercurrent flow relative to the  $F_1/F_2$  interface (e.g., Fig. 1(b) with  $\vec{H} = 0$ ). Figure 2 reveals that the induced  $y$ -component is present over the entire junction width as exhibited by the curved quasiparticle current trajectories. The spatial behavior of the triplet and singlet contributions to the supercurrent is also shown as a function of  $y$  (along the junction width) at four  $x$  locations along the junction length. The top and bottom set of panels corresponds to the current in the  $x$  and  $y$  directions respectively. The singlet and triplets components to the supercurrent both play important roles in the supercurrent: The amplitude of  $J_y^{s0}$  is comparable to  $|J_y^{sy} + J_y^{sz}|$ . These components of  $J_y$ , and hence  $J_y$  itself, vanish at  $y = 0, 2.0\xi_S$ , corresponding to the vacuum borders. The vector plot of the supercurrent density

FIG. 2. Spatial map of the critical current density  $\vec{J}(x, y)$  and its even- and odd-frequency components. The configuration of the  $S/F_1/F_2/S$  Josephson junction considered here is shown in Fig. 1(a). The junction length  $d_F$  is equal to  $2.0\xi_S$  and the width of each ferromagnetic strip labeled  $F_1$  and  $F_2$  are unequal, i.e.,  $W_{F1}=0.3\xi_S$  and  $W_{F2}=1.7\xi_S$ . Vertical lines in the panels separate the two ferromagnetic regions along the  $y$  direction.



in Fig. 2 reveals that the current flow in the middle of the junction ( $x=\xi_S$ ) is directed entirely along the  $x$ -direction throughout the junction width. The  $x$ -component of the singlet contribution to the current,  $J_x^{s0}$ , becomes vanishingly small when approaching this central region. On the contrary, the triplet contributions  $J_x^{sy}$  and  $J_x^{sz}$  are maximal there, demonstrating optimal singlet-triplet conversion. Another important aspect of this type of junction is seen in the behavior of  $J_x^{sy}$  and  $J_x^{sz}$  as a function of  $y$ : these triplet components generated in one  $F$  region penetrate deeply into the adjacent  $F$  segment. Therefore, two important phenomena arise: First, a singlet supercurrent flowing parallel to the interface of the  $F_1/F_2$  bilayers is converted into a triplet supercurrent of both spin projections. Second, there is a deep penetration of odd-frequency triplet supercurrents laterally (along  $y$ ) into the  $F$  wires possessing orthogonal magnetizations relative to the spin projection of the triplet supercurrents. The signatures of long-ranged proximity effects on the critical supercurrents flowing across similar structures as Fig. 1(a) are studied in Ref. 12. The planar structures with domain wall patterns are also investigated in Ref. 9 where the textured magnetizations generate long-ranged supercurrents regardless of either ‘transverse’ or ‘parallel’ transports [6]. We note that the results of Refs. 12 and 9 also fully confirm the generic scenario introduced here.

Next we illustrate an  $S/F_1/F_2/S$  junction depicted in Fig. 1(b). In Fig. 3(a), the external magnetic flux is absent, while in (b) a magnetic flux  $\Phi=3\Phi_0$  is applied to the system. The geometric dimensions correspond to  $d_{F1}=0.3\xi_S$ ,  $d_{F2}=1.7\xi_S$ , and the junction width,  $W_F=2.0\xi_S$ . In the absence of an external magnetic field, the charge supercurrent has no component along the  $y$  direction [15, 16, 20], and is constant along  $x$  (the supercurrent flows transverse to the  $F/F$  interface [14]). The relevant charge supercurrent density components,  $J_x^{s0}$ ,  $J_x^{sy}$ , and  $J_x^{sz}$ , thus only vary spatially in the  $x$  direction and their behaviors are substantially different from their counterparts where the supercurrent flows parallel to the  $F_1/F_2$  interface [Fig. 1(a) setup] shown in Fig. 2. It is evident that  $J_x^{sy}$  disappears in  $F_2$  while  $J_x^{sz}$  is zero inside the  $F_1$  segment since we have the exchange fields  $\vec{h}_1=(0, h^y, 0)$ , and  $\vec{h}_2=(0, 0, h^z)$  acting effectively as triplet spin filters. In other words,  $J^{sy}$  is generated in  $F_1$ , becomes localized there and then at the  $F_1/F_2$  interface, converts to the short-ranged  $J^{sz}$

in  $F_2$  (or vice versa). The triplet supercurrent generated in one  $F$  is closely linked to the local magnetization texture and therefore does not penetrate into the other  $F$  whose magnetization is orthogonal to the spin direction [13, 14, 19]. Turning now to Fig. 3(b), a magnetic field is applied, corresponding to a magnetic flux of  $\Phi=3\Phi_0$ . This induces proximity vortices that result in a nonuniform supercurrent response varying in both the  $x$  and  $y$  directions [15, 16, 20]. The corresponding supercurrent constituents,  $J_x^{s0}(x, y)$ ,  $J_y^{sy}(x, y)$ , and  $J_y^{sz}(x, y)$ , are thus also nonzero along  $y$ . The amplitude of  $J_x^{sy}(x, y)$ , is smaller than the other components due in part to the small  $F_1$  width,  $d_{F1}=0.3\xi_S$ , consistent with Fig. 3(a).

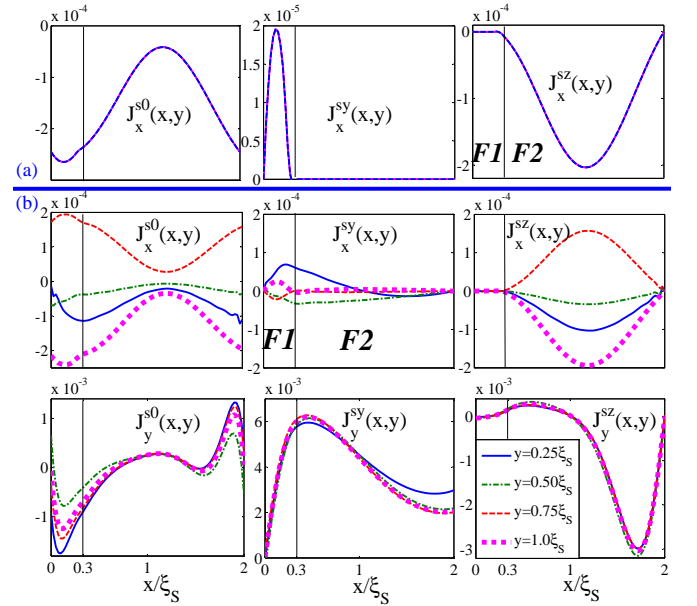


FIG. 3. Decomposed components of critical supercurrent density in an  $S/F_1/F_2/S$  junction depicted in Fig. 1(b). The two ferromagnetic strips have unequal lengths:  $d_{F1}=0.3\xi_S$ , and  $d_{F2}=1.7\xi_S$ , while their widths are equal:  $W_{F1}=W_{F2}=2.0\xi_S$ . In part (a), there is no applied magnetic field, whereas in part (b) the external magnetic field corresponds to a flux of  $\Phi=3\Phi_0$ . The critical current components in both cases, (a) and (b), are plotted as a function of  $x$ -position at four different locations along the junction width:  $y=0.25\xi_S$ ,  $0.50\xi_S$ ,  $0.75\xi_S$ ,  $1.0\xi_S$ .

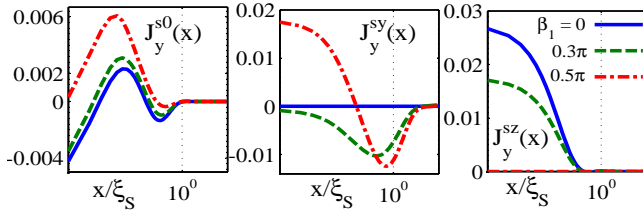


FIG. 4. Spatial behavior of decomposed diamagnetic supercurrent as a function of lateral position inside the  $S/F_1/F_2/N$  junction depicted in Fig. 1(c). Three magnetization orientations of  $F_1$  are shown:  $\beta_1=0, 0.3\pi$ , and  $0.5\pi$  ( $\alpha_1=\pi/2$ ), while  $F_2$  remains magnetized along  $z$  ( $\beta_2=0$ ). The thickness of the left  $F_1$  layer is fixed at  $d_{F1}=0.1\xi_S$ , while the thickness of the right  $F_2$  layer and  $N$  metal are  $d_{F2}=1.9\xi_S$  and  $d_N=2.5\xi_S$ .

As seen,  $J_x^{sz}(x, y)$ , is drastically suppressed at the  $F_1/F_2$  interface, similar to the case in Fig. 3(a). Examining the singlet and triplet components to the supercurrent flowing in the  $y$ -direction, we see that their contribution has increased dramatically compared to propagation in the  $x$  direction (nearly an order of magnitude or more). The overall spatial behavior of the even-frequency triplet components are different: The component with orthogonal spin projection to the magnetization direction  $J_y^{sy}(x, y)$  penetrates now extensively into the ferromagnetic regions compared with its  $x$ -component counterparts and the component with parallel spin projection,  $J_y^{sz}(x, y)$ . We note that the magnetization direction in  $F_2$  is orthogonal to the spin polarization of the  $J^{sy}$  supercurrent component. By considering these findings together with those of a  $S/F_1/F_2/S$  configuration where the  $F_1/F_2$  interface is orthogonal to the  $S/F$  interface in Fig. 2, and the results of Refs. 12 and 9, one concludes that: A singlet supercurrent flowing parallel to the interface of a simple  $F_1/F_2$  bilayer with noncollinear exchange directions, can significantly convert to a long-ranged spin-triplet supercurrent *regardless* of actual geometry.

To further explore the generality of the phenomenon and provide an experimentally accessible platform to isolate it, Fig. 4 exhibits the diamagnetic supercurrent in a  $S/F_1/F_2/N$  structure [Fig. 1(c)] with  $d_{F2}(=1.9\xi_S) \gg d_{F1}(=0.1\xi_S)$  and  $d_N=2.5\xi_S$ , at three magnetization orientations of  $F_1$ :  $\alpha_1=\pi/2$ ,  $\beta_1=0, 0.3\pi$ , and  $0.5\pi$ , while  $\vec{h}_2$  points along the  $z$  direction;  $\beta_2=0$ . As seen,  $J_y^{sy}$  flowing along the  $y$  direction, deeply penetrates  $F_2$  laterally. Whereas, the singlet  $J_y^{s0}$  and triplet  $J_y^{sz}$  components are short-ranged and drop drastically midway through the magnet region. Hence, here is a clear and practical opportunity to generate extensive long-range spin-triplet supercurrents by parallel supercurrent flow relative to the interface of a uniformly magnetized  $F_1/F_2$  structure with inequivalent  $F$  strips. The  $S/F_1/F_2/N$  structures proposed here are not only relatively simple to fabricate and readily accessible to experimental measurements [21], but they also serve as an efficient means to create samples for probing the previously discussed generic situations. In effect, the long-range triplet components deeply penetrate laterally into the

thick  $N$  region with minimal decay [14] while the singlet and short-range triplet supercurrent components nearly vanish by the time they reach the  $N$  layer. Therefore, this pure long-range triplet current, which is odd in frequency, can be experimentally isolated in very simple  $S/F_1/F_2/N$  structures. Considering today's technological advancements, the experimental investigation of the addressed phenomena in this Letter are readily accessible [21].

We would like to thank G. Sewell for valuable instructions in the numerical parts of this work. We also appreciate N.O. Birge for useful conversations and comments. K.H. is supported in part by ONR and by a grant of supercomputer resources provided by the DOD HPCMP.

\* [phymalidoust@gmail.com](mailto:phymalidoust@gmail.com)

† [klaus.halterman@navy.mil](mailto:klaus.halterman@navy.mil)

- [1] I. Zutic, J. Fabian, and S.D. Sarma, *Rev. Mod. Phys.* **76**, 323 (2004).
- [2] T. Kimura, Y. Otani, T. Sato, S. Takahashi, and S. Maekawa *Phys. Rev. Lett.* **98**, 156601 (2007).
- [3] A.G. Golubov, M.Y. Kupriyanov, and E. Ilchev, *Rev. Mod. Phys.* **76**, 411 (2004).
- [4] A.I. Buzdin, *Rev. Mod. Phys.* **77**, 935 (2005).
- [5] C.H.L. Quay, D. Chevallier, C. Bena, and M. Aprili, *Nat. Phys.* **9**, 84 (2013); F. Hubler, M.J. Wolf, D. Beckmann, and H.V. Lohneysen, *Phys. Rev. Lett.* **109**, 207001 (2012).
- [6] F.S. Bergeret, A.F. Volkov, and K.B. Efetov, *Rev. Mod. Phys.* **77**, 1321 (2005).
- [7] R.S. Keizer, S.T.B. Goennenwein, T.M. Klapwijk, G. Miao, G. Xiao and A. Gupta, *Nat.* **439**, 825 (2006).
- [8] M. Houzet and A.I. Buzdin, *Phys. Rev. B* **76**, 060504(R) (2007).
- [9] Y.V. Fominov, A.F. Volkov, and K.B. Efetov, *Phys. Rev. B* **75**, 104509 (2007).
- [10] T.S. Khaire, M.A. Khasawneh, W.P. Pratt Jr., and N. Birge, *Phys. Rev. Lett.* **104**, 137002 (2010).
- [11] J.W.A. Robinson, J.D.S. Witt, and M.G. Blamire, *Science* **329**, 5987 (2010); M. Alidoust, and J. Linder, *Phys. Rev. B* **82**, 224504 (2010).
- [12] T.Y. Karinskaya, M.Y. Kupriyanov, and A.A. Golubov, *JETP Lett.* **87**, 570 (2008); A.I. Buzdin, A.S. Melnikov, and N.G. Pugach, *Phys. Rev. B* **83**, 144515 (2011).
- [13] M. Houzet, A. I. Buzdin, *Phys. Rev. B* **74**, 214507 (2006); L. Trifunovic, *Phys. Rev. Lett.* **107**, 047001 (2011); L. Trifunovic, Z. Popovic, and Z. Radovic, *Phys. Rev. B* **84**, 064511 (2011).
- [14] M. Alidoust, and K. Halterman, A detailed paper including analytics and numerics: to be published (2015).
- [15] M. Alidoust, G. Sewell, and J. Linder, *Phys. Rev. Lett.* **108**, 037001 (2012).
- [16] M. Alidoust, and J. Linder, *Phys. Rev. B* **87**, 060503(R) (2013).
- [17] K.D. Usadel, *Phys. Rev. Lett.* **25**, 507 (1970).
- [18] M.Y. Kupriyanov, *Sov. Phys. JETP* **67**, 1163 (1988).
- [19] B. Crouzy, S. Tollis, D.A. Ivanov *Phys. Rev. B* **75**, 054503 (2007); *ibid* **76**, 134502 (2007).
- [20] J.C. Cuevas and F.S. Bergeret, *Phys. Rev. Lett.* **99**, 217002 (2007).
- [21] X.L. Wang, *et al.*, *Phys. Rev. B* **89**, 140508(R) (2014).